Thiol-Frozen Shape Evolution of Triangular Silver Nanoplates

Xuchuan Jiang, Qinghua Zeng, and Aibing Yu*

School of Materials Science and Engineering, University of New South Wales, Sydney, NSW 2052, Australia

Received September 25, 2006. In Final Form: November 22, 2006

The structural and optical stability of nanoparticles directly influences their applications. The shape evolution of silver nanoplates synthesized in the presence of bis(2-ethylhexyl) sulfosuccinate (AOT) could be effectively frozen using thiols in aqueous solution. These thiols (e.g., 1-hexanethiol, 1-octanethiol, 1-dodecanethiol, and 1-hexadecanethiol) exhibit stronger surface affinity on the silver crystalline surfaces. This is evidenced from both the unchanged shape/size of nanoplates and their unshifted plasmon resonances in optical absorption. To quantitatively explain the thiol-frozen shape evolution mechanism of silver nanoplates at molecular scale, molecular dynamics simulation was performed. The results show that these thiols exhibit larger interaction energies than AOT molecules on the silver atomic surfaces and hence freeze the shape evolution of silver nanoparticles. This thiol-frozen strategy would not only be useful for stabilizing nanoparticles but would also allow the introduction of a wide range of surface chemical functionalities to the nanoparticles for potential applications in nanosensors.

1. Introduction

The physicochemical properties of metal and semiconductor nanostructures dramatically depend on their morphologies and sizes.[1,2] Consequently, many attempts have been made in the past to explore the relationship between the structure and the property of nanomaterials that integrates the frontiers of physics, materials chemistry, and chemical engineering.[3−11] Metal nanoparticles have been widely investigated because of their unusual optoelectronic properties and potential applications in areas such as catalysis,[3] information storage,[4] biosensors,[5] and surface-enhanced Raman spectroscopy (SERS).[6] This is particularly true for precious metal (e.g., Au, Ag, Cu, Pt, and Pd) nanostructures. The optical properties of anisotropic nanostructures have been examined owing to their potential applications such as output signal enhancers in near-field optical microscopy[7] and as probes in biosensors.[8] Of the metallic nanostructures achieved thus far, silver is most attractive because of its superconductivity and intense colorimetric effect in nanoscale size. The performance of silver in most of these applications could be significantly enhanced by processing silver into well-defined dimensions. Two-dimensional (2-D) silver nanostructures have been extensively studied because of their remarkable abilities in tuning optical properties. As a result, a wealth of thermo- and photochemical approaches have been employed to fabricate silver 2-D nanostructures such as nanoplates,[9] nanoprisms,[10] and nanodiscs.[11] These nanostructures display a strong ultraviolet−visible (UV−vis) extinction frequency that is not present in the spectrum of the bulk metal. Their peak wavelength and localized surface plasma resonance are significantly dependent on their morphology, size, interparticle spacing, intrinsic dielectric properties, and local environment including solvents, substrates, and adsorbates.[6a,b] Any changes of these parameters could lead to the optical drift in absorption spectrum and thus influence the optical applications in practice. Therefore, the nanoparticle stability in solution is important.

To obtain stable nanoparticles, surfactants serving as capping ligands are often present in a synthesis process. These molecules can not only lead to uniform-size particles but can also prevent their aggregation or precipitation in solution.[10−12] For instance, Yin and Alivisatos[10a] discussed the influence of the capping

* To whom correspondence should be addressed. Tel: +61-2-93854429. Fax: +61-2-93855956. E-mail: a.yu@unsw.edu.au.

(1) (a) Kubo, R.; Kawabata, A.; Kobayashi, S. *Annu. Rev. Mater. Sci.* **1984**, *14*, 49−66. (b) *Ultra-Fine Particles-Exploratory Science and Technology;* Hayashi, C., Uyeda, R., Tasaki, A., Eds.; William Andrew Publishing: Noyes, NJ, 1997. (c) Perenboom, J.; Wyder, P.; Meier, F. *Phys. Rep.* **1981**, *78*, 173−292. (d) Nagaev, E. L. *Phys. Rep.* **1992**, *222*, 199−307.

(2) (a) Gaponenko, S. V. *Optical Properties of Semiconductor Nanocrystals;* Cambridge University Press: Cambridge, U.K., 1998. (b) Woggon, U. *Optical Properties of Semiconductor Quantum Dots;* Springer-Verlag: Berlin, 1997. (c) Kastner, M. A. *Phys. Today* **1993**, *46*, 24−31. (d) Alivisatos, A. P. *Science* **1996**, *271*, 933−937. (e) Brus, L. *J. Phys. Chem. Solids* **1998**, *59*, 459−465.

(3) (a) El-Sayed, M. A. *Acc. Chem. Res.* **2001**, *34*, 257−264. (b) Kamat, P. V. *J. Phys. Chem. B* **2002**, *106*, 7729−44.

(4) Sun, S.; Murray, C. B.; Weller, D.; Folks, L.; Moser. A. *Science* **2000**, *287*, 1989−92.

(5) Nicewarner-Peña, S. R.; Freeman, R. G.; Reiss, B. D.; He, L.; Peña, D. J.; Walton, I. D.; Cromer, R.; Keating, C. D.; Natan, M. J. *Science* **2001**, *294*, 137−141.

(6) (a) Dick, L. A.; McFarland, A. D.; Haynes, C. L.; Van Duyne, R. P. *J. Phys. Chem. B* **2002**, *106*, 853−60. (b) Kelly, K. L.; Coronado, E.; Zhao, L. L.; Schatz, G. C. *J. Phys. Chem. B* **2003**, *107*, 668−77. (c) Nie, S.; Emory, S. R. *Science* **1997**, *275*, 1102−06.

(7) (a) Link, S.; El-Sayed, M. A. *J. Phys. Chem. B* **1999**, *103*, 8410−26. (b) Kottmann, J. P.; Martin, O. J. F.; Smith, D. R.; Schultz. S. *Chem. Phys. Lett.* **2001**, *341*, 1−6. (c) Silva, T. J.; Schultz, S.; Weller, D. *Appl. Phys. Lett.* **1994**, *65*, 658−60.

(8) Schultz, S.; Smith, D. R.; Mock, J. J.; Schultz, D. A. *Proc. Natl. Acad. Sci. U.S.A.* **2000**, *97*, 996−1001.

(9) (a) Callegari, A.; Tonti, D.; Chergui, M. *Nano Lett.* **2003**, *3*, 1565−68. (b) Yener, D. O.; Sindel, J.; Randall, C. A.; Adair, J. H. *Langmuir* **2002**, *18*, 8692−99.

(10) (a) Yin, Y.; Alivisatos, P. *Nature* **2005**, *437*, 664−70. (b) Jin, R. C.; Cao, Y. W.; Mirkin, C. A.; Kelly, K. L.; Schatz, G. C.; Zheng, J. G. *Science* **2001**, *294*, 1901−03. (c) Jin, R. C.; Cao, Y.; Metraux, G. S.; Schatz, G. C.; Mirkin, C. A. *Nature* **2003**, *425*, 487−490. (d) Pastoriza-Santos, I.; Liz-Marzan, L. M. *Nano Lett.* **2002**, *2*, 903−905. (e) Metraux, G. S.; Cao, Y.; Jin, R. C.; Mirkin, C. A. *Nano Lett.* **2003**, *3*, 519−522.

(11) (a) Germain, V.; Li, J.; Ingert, D.; Wang, Z.; Pileni, M. P. *J. Phys. Chem. B* **2003**, *107*, 8717−20. (b) Maillard, M.; Giorgio, S.; Pileni, M. P. *Adv. Mater.* **2002**, *14*, 1084−86. (c) Maillard, M.; Giorgio, S.; Pileni, M. P. *J. Phys. Chem. B* **2003**, *107*, 2466−70. (d) Sun, Y.; Xia. Y. *Adv. Mater.* **2003**, *15*, 695−99. (e) Jiang, L.; Xu, S.; Zhu, J. M.; Zhang, J.; Zhu, J. J.; Chen, H. *Inorg. Chem.* **2004**, *43*, 5877−83.

(12) (a) Chen, S.; Carroll, D. L. *Nano Lett.* **2002**, *2*, 1003−07. (b) Murphy, C. J.; Jana, N. R. *Adv. Mater.* **2002**, *14*, 80−82. (c) Nikoobakht, B.; El-Sayed, M. A. *Chem. Mater.* **2003**, *15*, 1957−62. (d) Pérez-Juste, J.; Liz-Marzán, L. M.; Carnie, S.; Chan, D. Y. C.; Mulvaney, P. *Adv. Funct. Mater.* **2004**, *14*, 571−579. (e) Hu, J.; Chen, Q.; Xie, Z.; Han, G.; Wang, R.; Ren, B.; Zhang, Z.; Tian, Z. *Adv. Funct. Mater.* **2004**, *14*, 183−189. (f) Liz-Marzan, L. M.; Giersig, M.; Mulvaney, P. *Langmuir* **1996**, *12*, 4329−35. (g) Porel, S.; Singh, S.; Radhakrishnan, T. P. *Chem. Commun.* **2005**, 2387−88. (h) Hao, E.; Kelly, K. L.; Hupp, J. T.; Schatz, G. C. *J. Am. Chem. Soc.* **2002**, *124*, 15182−3. (l) Jiang, X. C.; Pileni, M. P. *Colloids Surf., A* **2006**, *277*, 201−206. (j) Brioude, A.; Jiang, X. C.; Pileni, M. P. *J. Phys. Chem. B* **2005**, *109*, 13138−42.

10.1021/la062797z CCC: $37.00
Published on Web 01/06/2007

molecules on the morphology of nanoparticles. Such molecules binding to nanocrystal surface via covalent or ionic bonds can influence the nucleation and growth along with spatially stabilizing the nanocrystals through passivating surface electronic states.[13] Various capping ligands have been employed in the previous studies, including bis(*p*-sulfonatophenyl) phenylphosphine dehydrate potassium for silver nanoprisms during the photoinduced conversion of tiny silver nanospheres,[10b−c] sodium bis(2-ethylhexyl) sulfosuccinate (NaAOT) molecules for truncated silver nanodiscs in isooctane by forming reverse micelles,[11a−c] cetyltrimethylammonium bromide (CTAB) for truncated silver triangles,[12a] trioctylphosphine oxide (TOPO) for CdSe nanocrystals at high temperature through passivation of lonely electron pair,[13] and poly(vinyl pyrrolidone) (PVP) for silver nanowires and nanocubes via adsorption on silver atomic surfaces.[14] Most of the methods focused on the shape control of particles at the initial stage. To date, little attention has been paid on the stability of nanostructures during their storage. The structural and optical stability of nanoparticles directly influences their applications. For example, the plasmon-enhanced spectroscopy requires stable and well-defined resonances. A shift of plasmon resonance, even if only a few nanometers, can reduce signal intensities by orders of magnitude, particularly if nonlinear optical enhancements are involved.[15] This is an important problem that should be properly addressed.

In this work, we demonstrated a convenient and effective method, that is, thiol-frozen approach, to stabilize triangular silver nanoplates synthesized using a self-seeding coreduction method in our recent study.[16] The size of the nanoplates capped with AOT molecules was ∼1.6 nm in thickness and ∼70 nm in edge length. During their storage at room temperature (∼25 °C), we found that the solution color of the as-synthesized nanoplates gradually changed, and correspondingly there was a shift of plasmon resonance in the optical absorption. To stabilize the triangular silver nanoplates, thiols with different lengths of carbon chain (e.g., $C_nH_{2n+1}SH$, $n = 6$, 8, 12, and 16) were used because of their strong affinity of −SH group on heavy metals (e.g., Au, Ag, and Cu) in their ions and metallic states.[17] The thiol-frozen silver nanoplates can provide stable plasmon resonances by modulating the dielectric function at the nanoplate surface and are stable for months without degradation at room temperature. Such a thiol-frozen approach would be useful for stabilizing heavy metallic nanoparticles that can be used as good candidates for chemical sensors.

2. Experimental Section

2.1. Chemicals. The as-received silver nitrate ($AgNO_3$, 99.9%), citrate acid (99%), L-ascorbic acid (≥99.0%), sodium borohydride ($NaBH_4$, 99%), sodium bis(2-ethylhexyl) sulfosuccinate (NaAOT, 99%), 1-hexanethiol ($C_6H_{13}SH$), 1-octanethiol ($C_8H_{17}SH$), 1-dodecanethiol ($C_{12}H_{25}SH$), and 1-hexadecanethiol ($C_{16}H_{33}SH$), all purchased from Sigma-Aldrich, were used in this work. All the solutions were freshly made for the synthesis and thiol treatment of silver nanoplates, and the $NaBH_4$ aqueous solution was ice-bathed. Milli-Q water was used in all the synthesis processes. All glassware was cleaned with aqua regia, was thoroughly rinsed with Milli-Q water, and was dried prior to use.

2.2. Synthesis of Silver Nanoplates. The synthesis of silver nanoplates mainly followed the procedures described in our recent study.[16] It was conducted at room temperature (∼25 °C). In a typical procedure, three steps were involved. First, 5.0 mL of aqueous $AgNO_3$ (0.01 M) and 5.0 mL of NaAOT (0.02 M) solution were added to a 250-mL conical flask, then Milli-Q water was added to the flask, and the final volume of the mixture was fixed to 200 mL, which was followed by stirring for around 10 min. Second, 0.67 mL of citrate acid (0.10 M) and 0.56 mL of L-ascorbic acid (0.10 M) freshly made aqueous solution were quickly added to the mixed solution containing Ag^+ ions and AOT, followed by vigorously stirring for ∼1 min. Finally, 10.0 μL of ice-bathed aqueous $NaBH_4$ solution (0.01 M) was quickly added to the above mixed solution and was stirred for about 30 s. Gradually, the color of the solution changed from light yellow to purple, pink, green, and dark blue over about 10 min, in which the as-prepared silver nanoplates formed.

2.3. Thiol Treatment of Silver Nanoplates. To stabilize the as-prepared silver nanoplates, thiols with different carbon-chain lengths (e.g., C_6, C_8, C_{12}, and C_{16}) were employed in this study. The as-received chemicals were used without any further purification. Here, different concentrations of thiol-ethanol solutions (e.g., 0.01, 0.03, 0.06, 0.10, and 0.20 M) were tested, but 0.10 M was used typically. Three steps were involved in the measurement of UV−vis spectrum of thiol-frozen silver nanoplates as follows. First, 10 mL of aqueous solution containing silver nanoplates was taken out from the 250-mL flask and was ejected into a 25-mL vial. This procedure was repeated four times, so as to produce five vials labeled as A, B, C, D, and E. Second, 0.10 mL of $C_6H_{13}SH$, $C_8H_{17}SH$, $C_{12}H_{25}SH$, and $C_{16}H_{33}SH$-ethanol solution (0.10 M) was added into four vials B, C, D, and E (not vial A which was used as a reference sample), followed by vigorously stirring for ∼10 min. To prevent the aggregation and precipitation of colloids, the replaced AOT was not removed from the thiol-treated solution during measuring the optical absorption. Finally, 2.5 mL of aqueous solution was separately taken out from each of the vials (A−E) and was ejected into a 1-cm quartz cell for the measurement of UV−vis spectrum. Other measurements of the thiol-frozen silver nanoplates were performed following the same procedures. All the thiol-frozen solutions of silver nanoparticle were stored at room temperature (∼25 °C).

2.4. Characterization. The microstructure and composition of silver nanoplates were measured under Philips CM200 field emission gun transmission electron microscope (TEM), operated at the accelerate voltage of 200 kV. The specimen was prepared by dropping the nanoplate solution onto Formvar-coated copper grids and then was dried in air naturally. The profile of silver nanoplates was measured by a Digital Instrument 3000 atomic force microscope (AFM). The X-ray diffraction (XRD) pattern was recorded using Siemens D5000 at a scanning rate of 0.5°/min in the 2θ range of 30−85°. Ultraviolet−visible (UV−vis) absorption spectrum was obtained on a CARY 5G UV−vis spectrophotometer (Varian) with a 1-cm quartz cell.

2.5. Molecular Dynamics Simulation. Molecular dynamics (MD) simulation with NVT (constant number of atoms, volume, and temperature) ensemble was performed to understand the formation and stability mechanisms of silver nanoplates. The simulation method and structural analysis were similar to the previous studies.[18] All simulations were performed using the Discover Module of Materials Studio (version 3.2, Accelrys Inc., 2005). The interaction energies between surfactant molecules (e.g., AOT and thiol) and three silver crystalline planes (i.e., 111, 110, and 100) were calculated. The

(13) (a) Murray, C. B.; Norris, D. J.; Bawendi, M. G. *J. Am. Chem. Soc.* **1993**, *115*, 8706−15. (b) Kuno, M.; Lee, J. K.; Dabbousi, B. O.; Mikulec, F. V.; Bawendi, M. G. *J. Chem. Phys.* **1997**, *106*, 9869−82. (c) Murray, C. B.; Kagan, C. R.; Bawendi, M. G. *Science* **1995**, *270*, 1335−38.

(14) (a) Sun, Y.; Mayers, B.; Xia, Y. *Nano Lett.* **2003**, *3*, 675−79. (b) Sun, Y.; Xia, Y. *Science* **2002**, *298*, 2176−79.

(15) (a) Wei, A. In *Nanoparticles: Scaffolds and Building Blocks*; Rotello, V. M., Ed.; Kluwer Academic: New York, 2004; pp 173−200. (b) Genov, D. A.; Sarychev, A. K.; Shalaev, V. M.; Wei, A. *Nano Lett.* **2004**, *4*, 153−8. (c) Imura, K.; Nagahara, T.; Okamoto, H. *J. Am. Chem. Soc.* **2004**, *126*, 12730−31.

(16) Jiang, X. C.; Zeng, Q. H.; Yu, A. B. *Nanotechnology* **2006**, *17*, 4929−35.

(17) (a) Wierse, D. G.; Lohrengel, M. M.; Schultze, J. W. *J. Electroanal. Chem.* **1978**, *92*, 121−131. (b) Lezna, R. O.; de Tacconi, N. R.; Arvia, A. J. *J. Electroanal. Chem.* **1990**, *283*, 319−336. (c) *Adsorption on Metal Surfaces*; Benard, J., Ed.; Elsevier: Amsterdam, 1983. (d) Lay, M. D.; Varazo, K.; Stickney, J. L. *Langmuir* **2003**, *19*, 8416−27. (e) Levchenko, A. A.; Yee, C. K.; Moloy, E.; Parikh, A. N.; Navrotsky, A. *Chem. Mater.* **2005**, *17*, 5428−38. (f) Gupta, P.; Ulman, A.; Fanfan, S.; Korniakov, A.; Loos, K. *J. Am. Chem. Soc.* **2005**, *127*, 4−5.

(18) (a) Mayo, S. L.; Olafson, B. D.; Goddard, W. A., III. *J. Phys. Chem.* **1990**, *94*, 8897−8907. (b) Zeng, Q. H.; Yu, A. B.; Lu, G. Q.; Standish, R. K. *Chem. Mater.* **2003**, *15*, 4732−38.

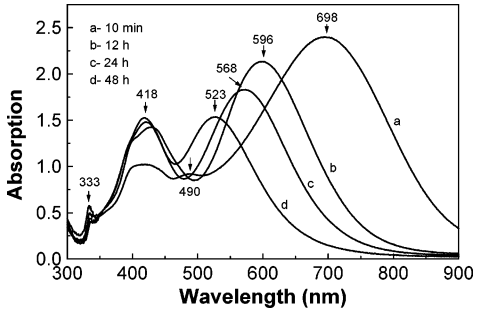

Figure 1. The shift of plasmon resonances of silver nanoplates in aqueous solution at (a) 10 min, (b) 12 h, (c) 24 h, and (d) 48 h.

representative system consisted of one silver crystalline plane and seven AOT molecules on the surface of silver. All the systems were subject to energy minimization for the structural optimization before MD simulation. All MD simulations last for 50 ps with a time step of 1 fs. Data were collected in the last 20 ps for statistical and structural analysis. Details of the MD simulation work (e.g., interaction energies, atom density profiles) have been discussed in our recent work.[19]

3. Results and Discussion

3.1. Shape Evolution and Its Effect on Plasmon Resonance. The shape evolution of the triangular silver nanoplates coated by AOT molecules could be observed from the shift of plasmon resonances in optical absorption. Figure 1 shows that the maximum plasmon resonance of silver nanoplates shifts toward shorter wavelength from 698 to 596, 568, and 523 nm corresponding to different stages: 10 min (a), 12 (b), 24 (c), and 48 h (d), respectively. The featured plasmon resonances of triangular silver nanoplates in Figure 1a are centered at 698, 490, 418, and 333 nm. Those centered at 698 and 490 nm could be assigned to in-plane dipolar and quadrupolar plasmon resonance, and the other two centered at 418 and 333 nm could be assigned to out-of-plane dipolar and quadrupolar ones, respectively. This is in good agreement with the simulation by using discrete dipole approximation (DDA) method.[10b,20,21]

The shift of plasmon resonances toward short wavelength appears to be quite sensitive to the morphology of silver nanoplates on the basis of the TEM observations (Figure 2). One representative TEM image of triangular silver nanoplates is shown in Figure 2A, in which the edge length of triangular nanoplates is around 70 nm. Over aging for a period of time, the silver nanoplates could gradually evolve to the intermediate of plates and discs around 12 h (Figure 2B) and 24 h (Figure 2C) and finally to circular plates ~48 h (Figure 2D) in aqueous media at room temperature. On the basis of the TEM observations, three typical shapes (e.g., triangle, intermediate, and disc) are displayed in Figure 3A. The crystalline-plane evolution is probably caused by surface atomic migration, and the possible mechanism is discussed below. The evolution of Ag(100) and Ag(110) could be schematically illustrated in Figure 3B, in which the Ag(111) is still maintained as the basal plane.

To prevent the shape evolution and to stabilize the silver nanoplates, we need to understand first their growth and evolution mechanisms in aqueous solution. Many efforts have been made to explore the formation mechanisms of silver 2-D nanostructures by using different surfactants in the past years.[11a−c, 12a] However, previous studies only provided qualitative description. To date,

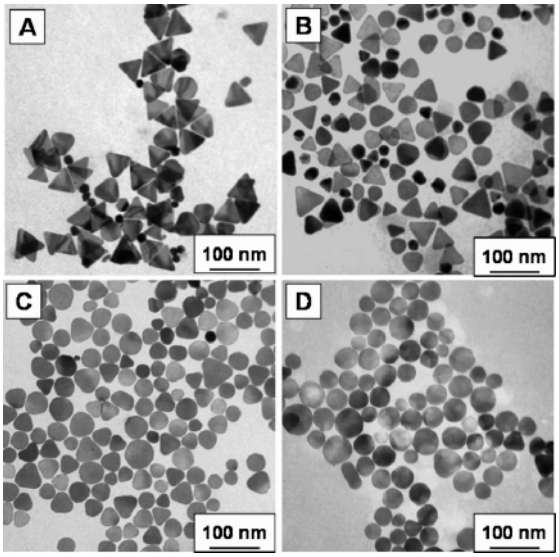

Figure 2. TEM images showing the evolution of silver nanoplates: (A) 10 min, (B) 12 h, (C) 24 h, and (D) 48 h.

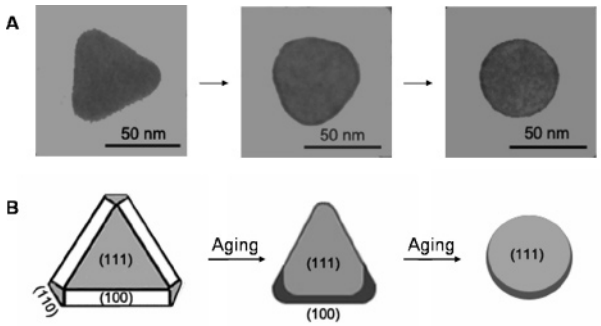

Figure 3. Typical TEM image of one silver nanoplate from triangular shape to intermediate between triangle and disc and then to a disc over aging (A) and a schematically diagram illustrating the evolution of silver atomic planes (B).

there is no generally accepted theoretical method for determining the interaction of organic surfactant molecules on the nanocrystal surface, so the choice of surfactant is very much empirical. Recently, we applied MD method to quantify the interaction potential energies between the AOT molecules and the silver atomic surfaces.[19] While useful, we would like to point out that the MD simulations are usually performed under conditions which may not fully represent the reality. Consequently, the resulting information should be used with caution, particularly in a quantitative way. The problem here is that it is difficult to obtain experimental results to confirm a simulation approach. Nevertheless, the MD results provide useful information to understand the fundamentals at a molecular level. For the systems considered in this work, we computed the interaction energies under comparable conditions so that their difference can be at least qualitatively used to explain the shape growth and evolution of silver nanoplates and the thiol-frozen mechanisms.

For each silver crystalline plane (i.e., 111, 110, or 100), simulations were performed on three models with the same MD cell dimension but with different components (i.e., silver plane with AOT molecules (A-B), isolated silver plane (A), and isolated AOT molecules (B)). The interaction potential energy represents the interaction strength of AOT molecules binding on silver planes. Such energy is calculated by the following equation: $\Delta U_{int} = U_{A-B} - U_A - U_B$, where U_{A-B}, U_A, and U_B are the potential energies of silver plane with AOT molecules (A-B), isolated silver plane (A), and isolated AOT molecules (B),

(19) Zeng, Q. H.; Jiang, X. C.; Yu, A. B.; Lu, G. Q. *Nanotechnology*, in press (available online at http://www.iop.org/EJ/journal/-page=forthart/0957-4484/1).
(20) Schatz, G. C.; Van Duyne, R. P. In *Handbook of Vibrational. Spectroscopy*; Chalmers, J. M., Griffiths, P. R., Eds.; Wiley: New York, 2002.
(21) Brioude, A.; Pileni, M. P. *J. Phys. Chem. B* **2005**, *109*, 23371−77.

respectively. The interaction potential energies of AOT molecules on the three silver atomic planes were calculated as {100} −249.9, {110} −323.4, and {111} −460.1 kcal/mol. Clearly, the Ag-{111}−AOT system is the most stable one among the three. These results can explain both the growth and the shape evolution mechanisms of silver nanoplates. The AOT molecules preferentially bind to the Ag(111) surface and impede its growth, and thus the fast growth in Ag(110) and Ag(100) planes would lead to the formation of platelike particles. Subsequently, the atomic migration on silver surfaces primarily occurs between Ag(100) and Ag(110) planes within individual particles because of the relatively small difference of interaction energies.

3.2. Thiol-Frozen Silver Nanoplates. The shape evolution would directly influence the optical stability and potential applications. So, there is a need to find a way to stabilize the triangular silver nanoplates, because optical applications involving plasmon-enhanced spectroscopes require the substrates with stable and well-defined resonance. Zweifel and Wei[22a] described the sulfide-arrested growth of gold nanorods in aqueous solution. The sulfide serves primarily as a scavenger for $AuCl_4^-$ and Ag^+ ions, removing them from the reaction mixture by reducing $AuCl_4^-$ ions with Na_2S to form Au or Ag_2S particles.[22b] However, their approach might lead to byproducts in stabilizing gold nanorods.

To reduce the possible byproducts (e.g., Ag_2S), in this work, thiols (i.e., $C_nH_{2n+1}SH$) including C_6, C_8, C_{12}, and C_{16} were chosen to modify the surface of silver nanoplates. It was found that a small amount of thiol (e.g., the mole ratio of thiol to silver is 4:1) could completely prevent the evolution of nanoplates. The solution of thiol-frozen nanoplates was stable at room temperature (∼25 °C) with no color change even after a couple of months. One typical TEM image of silver nanoplates stabilized by $C_{12}H_{25}SH$ over aging for 48 h is shown in Figure 4A. It is hard to identify any obvious changes in the morphology and size compared with those freshly synthesized triangular silver nanoplates (Figure 2A).

The microstructure of silver nanoplates was also investigated. The selected area electron diffraction (SAED) pattern of a triangular silver plate and its high-resolution TEM (HRTEM) image are displayed in Figure 4B and 4C, respectively. The spot-scattered SAED pattern clearly indicates that the silver plate is single crystalline, and the hexagonal symmetry of the scattered spots is an indication that the silver plate is highly [111] oriented with the top normal to the electron beam. The diffraction spots could be indexed according to the face-center-cubic (fcc) structure of silver. Three sets of diffraction spots could be indexed as (1/3){422} (circled spot), {220} (boxed spot), and {311} (spot circumscribed by triangle) on the basis of Bragg reflections associated with lattice spacing of around 2.50, 1.44, and 1.23 Å, respectively. The set of spots with a lattice spacing of ∼2.50 Å was believed to originate from the (1/3){422} plane normally forbidden by an fcc lattice. The appearance of the forbidden (1/3){422} plane is often observed on silver or gold nanostructures in the form of thin plates or films bound by atomically flat and bottom faces.[10b,11a,15] The fringe spacing ∼2.36 Å could be attributed to Ag(111) plane (Figure 4C), which reveals that the single crystalline silver plate is formed with the surface-bounded {111} planes. The thickness of silver nanoplates could be measured by atomic force microscopy (AFM). Figure 4D shows the profile of two silver nanoplates with top view, and the thickness of nanoplates was estimated ∼1.6 nm as pointed by the down triangle pairs (Figure 4E).

(22) (a) Zweifel, D. A.; Wei, A. *Chem. Mater.* **2005**, *17*, 4256−61. (b) Zhang, J.; Schwartzberg, A. M.; Norman, T., Jr.; Grant, C. D.; Liu, J.; Bridges, F.; Van Buuren, T. *Nano Lett.* **2005**, *5*, 809−810.

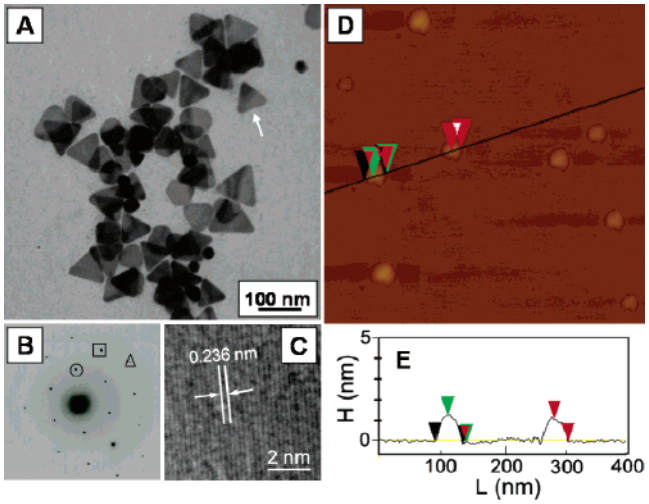

Figure 4. (A) TEM images of triangular silver nanoplates by treatment of $C_{12}H_{25}SH$ at 10 min, (B) the SAED pattern of one selected silver nanoplate in which the circled spot, boxed spot, and spot circumscribed by triangle corresponding to allowed (1/3){422}, {220}, and {311} Bragg reflections with lattice spacing of ∼2.5, ∼1.44, and ∼1.23 Å, respectively, (C) HRTEM image showing the lattice spacing ∼2.36 Å corresponding to Ag{111} plane, (D) the AFM image (top view), and (E) the thickness of nanoplates marked by down triangles.

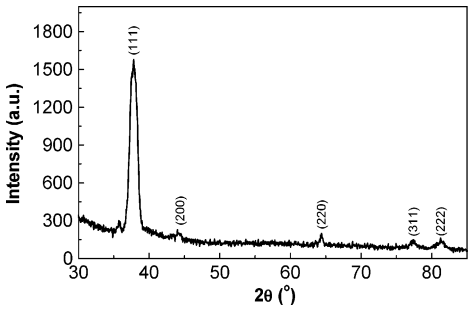

Figure 5. XRD pattern of silver nanoplates showing that Ag(111) plane is the basal one.

To gain more insights of the thiol-frozen silver nanoplates, the composition was recorded using powder X-ray diffraction (XRD). Figure 5 displays an XRD pattern of the thiol-frozen silver nanoplates, in which the diffraction peaks could be assigned to the (111), (200), (220), (311), and (222) planes of fcc silver rather than silver sulfide on the basis of the standard values in the card (JCPDS file no. 04−783).[23] The intensity ratios between (200) and (111) and between (220) and (111) planes are smaller than those conventional values (0.14 versus 0.4) and (0.12 versus 0.25), respectively. This indicates that the silver nanoplates were abundant in {111} facets, and their {111} planes tended to be preferentially oriented parallel to the surface of the supporting substrate.[11] The thiol-frozen silver nanoplates maintain the characteristic feature of atomically flat top and bottom.

MD simulation was again performed to understand the thiol-frozen mechanism of triangular silver nanoplates. It is believed that the strong affinity of −SH head groups on metals (e.g., Au, Ag, Cd, and Zn) could lead to intensive surface adsorption of thiol molecules on silver surfaces in this system.[24−28] This can be supported by the theoretical calculation using MD simulations. For example, the interaction energies between $C_{12}H_{25}SH$ molecules and silver atom surfaces were calculated on the basis

(23) Cullity, B. D.; Stock, S. R. *Elements of X−Ray Diffraction*, 3rd ed.; Prentice Hall: Upper Saddle River, NJ, 2001.

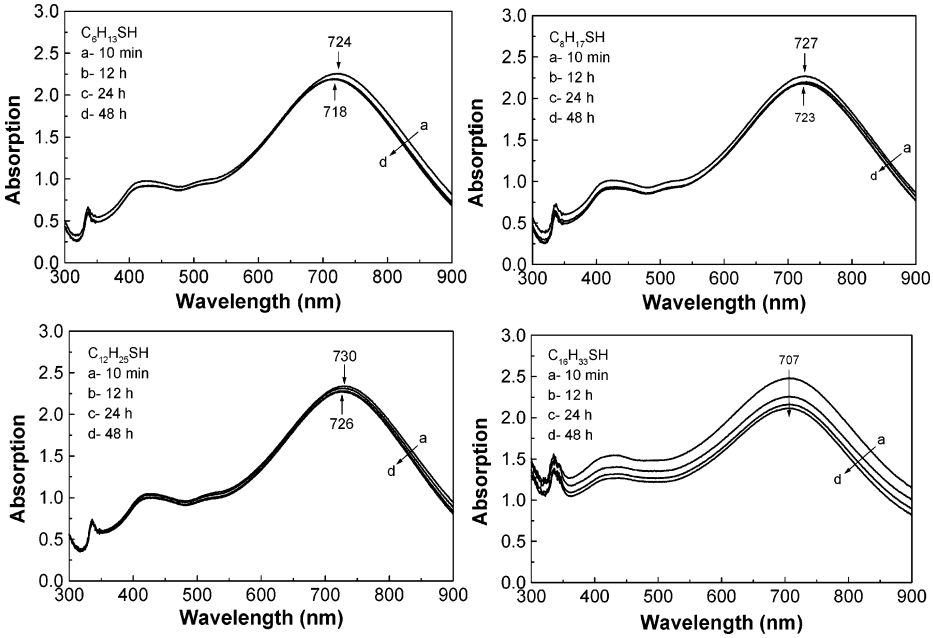

Figure 6. UV−vis spectra of the thiol-frozen silver nanoplates at different times of 10 min, 12, 24, and 48 h when using thiols (the molar ratio of thiol to silver is 4:1) with different carbon-chain lengths: (A) C_6, (B) C_8, (C) C_{12}, and (D) C_{16}.

of the simulation model in the previous studies.[18] The results are {100} −308.6, {110} −361.1, and {111} −959.0 kcal/mol, which indicates the thiol has much stronger interaction strength with Ag{111} plane than with other planes (e.g., 110, and 100). Comparing with AOT molecules, the binding ability of $C_{12}H_{25}$-SH to the silver surfaces is much stronger. However, it is also noted that the difference of interaction energies in binding of thiols to different silver surfaces (∼600 kcal/mol) is surprisingly high, which may not be realistic. Further work is necessary to examine this matter and the applicability of the proposed MD approach to this system.

To further understand the interactions, we calculated the interaction potential energy of both $C_{12}H_{25}SH$ and AOT bound to silver surface, such as Ag{100}. The interaction potential energy was around −104.6 kcal/mol, lower than sole AOT molecules after treated with $C_{12}H_{25}SH$. So, the surface treatment using thiol could largely increase the stability of silver nanoplates. We thought the interaction energies between the silver surfaces and capping molecules predominate the formation of silver nanoplates upon the adsorption of AOT or thiol molecules, although the surface energies in bare silver were driven to the formation of truncated octahedron for free clusters.[29]

3.3. Optical Absorption. Monitoring the plasmon resonance reveals that large improvements in optical stability have been achieved by addition of a small amount of thiols. The measurement of UV−vis spectra was performed by following the procedures described in the Experimental Section. After encapsulation with thiol, we did not take any steps to remove AOT from the solution

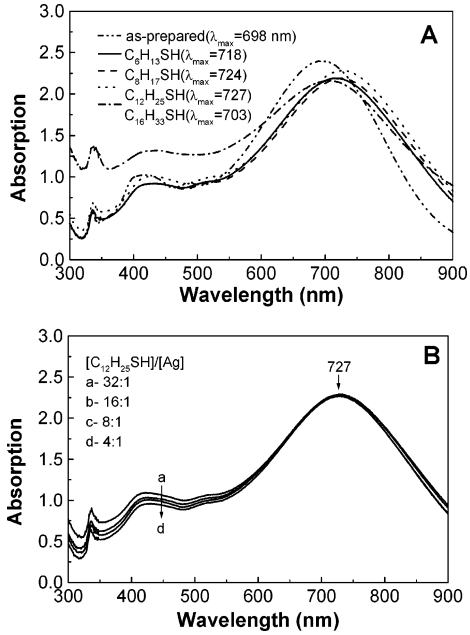

Figure 7. (A) UV−vis spectra of different thiol-frozen silver nanoplates over aging for 24 h: C_6 (solid line), C_8 (dot line), C_{12} (dash line), and C_{16} (dash dot line) with the same molar ratio of thiol to silver at 4:1; and (B) the influence of the molar ratios of $C_{12}H_{25}SH$ to silver over aging for 24 h: (a) 32:1, (b) 16:1, (c) 8:1, and (d) 4:1.

because the AOT still plays an important role in maintaining the stability of the whole system. Our experimental results indicate that the removal of AOT from the reaction system would lead to the aggregation and precipitation of silver nanoplates. Here, only a slight shift was found in plasmon resonance (Figure 6) after being treated with thiols (here, the molar ratio of thiol to silver was fixed at 4:1). This indicates that the thiols are very effective in stabilizing the nanoparticles. Compared with other thiols such as $C_6H_{13}SH$, $C_8H_{17}SH$, and $C_{16}H_{33}SH$, it is established that $C_{12}H_{25}SH$ can strongly bind to the silver surface on the basis of its maximum plasmon resonance, which is consistent with the previous studies.[24]

(24) (a) Prasad, B. L. V.; Stoeva, S. I.; Sorensen, C. M.; Klabunde, K. J. *Langmuir* **2002**, *18*, 7515−20. (b) Martin, J. E.; Wilcoxon, J. P.; Odinek, J.; Provencio, P. *J. Phys. Chem. B* **2000**, *104*, 9475−86.

(25) (a) McFarland, A. D.; Van Duyne, R. P. *Nano Lett.* **2003**, *3*, 1057−62. (b) Malinsky, M. D.; Kelly, K. L.; Schatz, G. C.; Van Duyne, R. P. *J. Am. Chem. Soc.* **2001**, *123*, 1471−82.

(26) (a) Sastry, M.; Lala, N.; Patil, V.; Chavan, S. P.; Chittiboyina, A. G. *Langmuir* **1998**, *14*, 4138−42. (b) Sastry, M.; Mayya, K. S.; Patil, V.; Paranjape, D. V.; Hegde, S. G. *J. Phys. Chem. B* **1997**, *101*, 4954−58.

(27) Weisbecker, C. S.; Merritt, M. V.; Whitesides, G. M. *Langmuir* **1996**, *12*, 3763−72.

(28) (a) Song, Y.; Huang, T.; Murray, R. W. *J. Am. Chem. Soc.* **2003**, *125*, 11694−701. (b) Ingram, R. S.; Hostetler, M. J.; Murray, R. W. *J. Am. Chem. Soc.* **1997**, *119*, 9175−78. (c) Ulman, A. *Chem. Rev.* **1996**, *96*, 1533−54.

(29) Balleto, F.; Ferrando, R. *Rev. Mod. Phys.* **2005**, *77*, 371.

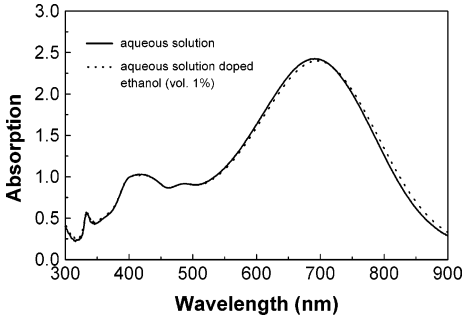

Figure 8. The influence of a small amount of ethanol (~1 vol %) for dissolving thiols in aqueous media on the optical absorption of the silver nanoplates without thiol treatment.

Further studies were done to examine the effects of the carbon-chain length of thiols, the molar ratio of thiols to silver, and the presence of ethanol on the optical absorption of silver nanoplates. Figures 7 and 8 show the results. Compared with the original solution of silver nanoplates, the maximum plasmon resonance of thiol-frozen nanoplates red-shifted around 20, 26, 31, and 8 nm corresponding to the thiols with different carbon-chain lengths, that is, C_6, C_8, C_{12}, and C_{16}, respectively (Figure 7A). This is probably due to the different electron-donating nature of −SH head groups in different thiols.[21] The maximum plasmon resonance of $C_{16}H_{33}SH$ had a slight blue shift compared with others, probably caused by the steric effect of 16-carbon chain when binding to the silver surfaces. Similarly, Martin et al.[24b] studied the lability of thiols with different carbon-chain lengths and found that $C_{16}H_{33}SH$ either do not stick to the Au nanocluster surfaces at all or are very labile.

It appears that the molar ratio of $C_{12}H_{25}SH$ to silver does not affect the optical absorption of silver nanoplates much. From the absorption spectra as shown in Figure 7B, the maximum plasmon resonance (λ_{max}= 727 nm) does not shift in position even though the molar ratio of $C_{12}H_{25}SH$ molecules to silver is decreased to 4. This indicates that even a small amount of thiol could stabilize the silver nanoplates.

(30) Henglein, A. *J. Phys. Chem. B* **1993**, *97*, 5457−71.

The effect of ethanol on the optical property of the thiol-frozen silver nanoplates should be tested because the ethanol still remained in the aqueous solution after binding thiol to silver surfaces. In fact, nanoparticles are sensitive to their local environment, that is, the surrounding solvent molecules.[25,30] Van Duyne and co-workers[25] reported the influence of solvents (e.g., nitrogen, methanol, 1-propanol, chloroform, and benzene) on the resonant Rayleigh scattering spectrum of single Ag nanoparticle. In the present system, a small amount of ethanol was used in thiol-frozen process to assist the dissolution of thiols because of the insolubility of thiols in water. The influence of ethanol was studied by adding 0.1 mL of absolute ethanol into 10 mL of aqueous solution containing silver nanoplates. As shown in Figure 8, the addition of such a small amount of ethanol (~1 vol %) does not change the color and the maximum plasmon resonance of the silver nanoplates. This confirmed that the presence of a small amount of ethanol, as used for dissolving thiols, would not affect the optical absorption of the thiol-frozen silver nanoplates.

4. Conclusions

The instability of triangular silver nanoplates coated with AOT molecules could be frozen using thiols because of their stronger affinity on the silver surface. The thiol-frozen mechanism can be explained using molecular dynamics method. By this simulation, the interaction potential energies between the thiol molecules and different silver surfaces were generated. The morphological and optical stability of the thiol-frozen silver nanoplates would make them attractive candidates as contrast agents for chemosensor and biosensor applications. This shape-frozen strategy would be useful for stabilizing the heavy metal nanoparticles and functionalizing their surface for potential applications in chemical and biochemical sensors.

Acknowledgment. This research was financially supported by the Australia Research Council (ARC) through ARC Center for Functional Nanomaterials.

LA062797Z